

Paper No.  
**105**

**MECHANISMS CONTRIBUTING TO ENHANCED CORROSION IN THREE PHASE SLUG  
FLOW IN HORIZONTAL PIPES**

**M. GOPAL, A. KAUL, AND W. P. JEPSON  
NSF, I/UCRC CORROSION IN MULTIPHASE SYSTEMS CENTER  
DEPARTMENT OF CHEMICAL ENGINEERING  
OHIO UNIVERSITY  
ATHENS, OHIO 45701  
USA**

**ABSTRACT**

Flow visualization experiments have been conducted in 7.5 cm and 10 cm I.D. three phase oil-water-gas pipes. The mechanisms that lead to increased corrosion rates in three-phase slug flow have been determined. The results show the existence of pulses of bubbles that have been formed in the mixing zone of the slug. These can impact on the lower pipe wall producing a cavitation-type effect leading to high rates of localized wall shear stress and associated high corrosion rates. This mechanism is sufficient to remove corrosion products and certain corrosion inhibitor films. The corrosion rate is strongly dependent on the flow composition and the Froude Number.

**KEYWORDS**

Corrosion / Erosion, Multiphase Slug Flow, Mixing Zone, Large Diameter Horizontal Pipeline, Bubble Impact, Wall Shear

**INTRODUCTION**

Long distance multiphase pipelines are becoming a significant mode of transportation for the oil and gas industry. It is more economical to combine the flow from several wells in a remote site, such as Alaska

**Publication Right**

Copyright by NACE International. NACE International has been given first rights of publication of this manuscript. Requests for permission to publish this manuscript in any form, in part or in whole must be made in writing to NACE International, Publications Division, P.O. Box 218340, Houston, Texas 77218-8340. The material presented and the views expressed in this paper are solely those of the author(s) and are not necessarily endorsed by the Association. Printed in the U.S.A.

or subsea, into a large diameter multiphase pipeline through which the mixture is transported to a platform or central gathering station. The mixture is then separated for future processing here.

In mature wells with enhanced oil recovery techniques, the amount of water produced increases significantly. The increased water cuts, combined with high carbon dioxide partial pressures, in the case of sweet wells, lead to highly corrosive internal environments.

In these multiphase pipes, several flow regimes can exist. These include stratified, slug, and annular flows. Most often, production rates involved in oil and gas result in slug flow conditions. The characteristics of slug flow increase corrosion/erosion effects resulting in rates much greater than those in other flow regimes.

Ellison and Wen<sup>1</sup> (1981) proposed three mechanisms for corrosion, convective mass transfer, phase transport, and erosion-corrosion. Erosion-corrosion often occurs at high velocity, turbulent flow, or when solids are present. The turbulent nature of the flow can enhance the mass transfer process while contributing to the removal of corrosion products from the pipe wall.

Sun and Jepson<sup>2</sup> (1992) and Zhou and Jepson<sup>3</sup> (1993) have demonstrated that there exist regions of high wall shear stresses and turbulence within the slug. Zhou and Jepson<sup>4</sup> (1994) found that the presence of gas at the bottom of the pipe in regions within the slug had significant effects on the corrosion rates. The result is a significant increase in corrosion rates. These results are also supported by Green et al.<sup>5</sup> (1990).

The flow characteristics in slugs have been studied by several workers, e.g., Dukler and Hubbard<sup>6</sup> (1975). A slug is initiated from stratified flow. Waves grow on the gas liquid interface and bridge the pipe to form a slug. This is accelerated to the velocity near that of the gas. The front of the slug rolls over the liquid film ahead of the slug and a highly turbulent mixing zone is created in which the liquid is assimilated into the slug. The mixing zone also entrains large amounts of gas. This is shown schematically in Figure 1. As the slug front rolls over the liquid film large amounts of gas and liquid are entrained into the mixing zone where a vortex is created (Dukler and Hubbard<sup>6</sup>, 1975). Some of the entrained gas is returned to the gas pocket ahead of the slug, while most of it is passed into the slug body.

Jepson<sup>7</sup> (1987) showed that slugs were propagating hydraulic jumps. He observed that the gas was entrained into the slugs in the form of pulses of bubbles. Zhou and Jepson<sup>4</sup> (1994) discussed possible mechanisms contributing to enhanced corrosion in slugs and found that the entrained pulses of gas bubbles were shot towards the bottom of the pipe. They found a strong correlation between corrosion rate and the amount of gas at the bottom of the pipe. Vuppu and Jepson<sup>8</sup> (1993) found impact craters in inhibitor films that could have been a result of the collapse of gas bubbles.

This work presents a video analysis of the nature of the flow within the mixing zone of the slug. It demonstrates the generation of pulses of bubbles and their existence at the bottom of the pipe. A possible relationship between the pulses of bubbles and wall shear stress is presented that could explain the enhanced corrosion rates observed in slug flow.

## EXPERIMENTAL SETUP

The test facility is similar to that described by Zhou and Jepson<sup>3,4</sup> (1993, 1994). It is shown schematically in Figure 2. The oil-water mixture is pumped from a 1.2 m<sup>3</sup> stainless steel storage tank into a 7.5 cm ID PVC pipe, where the liquid flowrate is measured by an orifice plate. The flow is allowed to expand into a 10 cm ID, 10 m Plexiglass pipeline. Carbon dioxide gas is introduced at the entrance of the Plexiglass pipe, and slugs are created here. The multiphase mixture flows through the Plexiglass pipeline and discharges into the liquid storage tank. The gas is separated by specially designed de-entrainment internals and is vented to the atmosphere, and the liquid is recirculated into the system.

Measurements of slug flow characteristics are made in the test section. The details of the test section are described in Figure 3. The wall shear stress is measured at position E, using flush mounted hot film sensors. The signals from the probe are passed to a TSI anemometry system for processing and stored on a PC. The descriptions of other measurements are given by Zhou and Jepson<sup>4</sup> (1994). Additional video analysis were conducted in a 7.5 cm I.D., 10 m long, Plexiglass pipeline, that was virtually identical to the 10 cm I.D. system.

All experiments were conducted at 40C and 0.137 Mpa carbon dioxide partial pressure.

Figure 4 shows a schematic of the flow visualization system used for the video analysis. The flow is observed from two different Super-VHS cameras. The signals from the cameras are passed to an audio-visual digital effects mixer, where they are combined into a single image. This is then sent to an industrial model S-VHS VCR are viewed on TV. Further image analysis could be performed by digitizing the images and transferring them to a SGI<sup>TM</sup> graphics workstation.

The fluids used in this study are ASTM D1141-52 seawater, a light condensate oil and carbon dioxide for corrosion studies. Deionized water is used to obtain high-resolution video images for close examination of the mechanisms in the mixing zone of the slug. The oil chosen is commonly used for simulating gas/condensate type flows. The density and viscosity of the oil at 40C is 825 kg/m<sup>3</sup> and 2 cp respectively.

Oil-water mixtures in the liquid phase ranging from 0% to 100% oil were studied. Slug flow was studied at velocities ranging from 3 to 4.5 and 6 m/s respectively. These were analyzed on the basis of Froude numbers (Sun and Jepson (1992), Zhou and Jepson (1994)) of 6, 9, and 12.

## RESULTS

Figures 5 through 9 show video images of the first 20 cm of a moving slug at a gas velocity of about 2.5 m/s, and liquid velocity of 0.4 m/s. The images are obtained at intervals of 0.017 s.

Figures 5 and 6 show a video image of the slug front viewed at an angle of 20° to the flow axis. It can be seen that the slug front is a propagating hydraulic jump associated with large amounts of aeration. A rolling motion associated with the slug front is also seen. This is associated with a mixing vortex that is generated just behind the front of the slug

The generation of pulses of gas bubbles can be seen from Figure 5. This is the mechanism of gas

entrainment into the mixing region of the slug. A region of gas-free liquid exists just after the mixing vortex. This is seen by the darker areas in Figure 5 and 6. As the frothy mixture ahead of the vortex touches the top of the pipe, the slug length is suddenly increased and the vortex moves towards the new front. This frees the liquid at the end of the vortex and it moves towards the body of the slug. As the movement starts, a pulse of bubbles is released to the right of this region. This pulse of gas bubbles is also mixed with the vortex, and is shot towards the bottom of the pipe. The bubbles impact on the pipe wall and can collapse, causing a cavitation-type effect, that can tear apart inhibitor films causing a degradation in performance.

Figures 7, 8 and 9 show video images of the mixing zone behind the slug front. The evidence of further pulses of bubbles can be clearly seen. Again, the liquid can be distinguished from the darker spots between the frothy pulses of gas. It is seen that there are large amounts of gas entrainment, and that the gas exists in frothy structures that are distributed across the entire depth of the pipe.

Figures 7 and 8 clearly show the existence of gas bubbles on the pipe wall. This proves that the pulses of gas bubbles are shot towards the bottom and can impact on the pipe wall causing a cavitation-type effect. Figures 7, 8 and 9 also illustrate the rolling motion associated with the slug front and the mixing zone. This can cause significant amounts of scouring and shear on the pipe wall.

The combination of scouring and shear due to the rolling motion, and the bubble impact on the pipe wall, results in corrosion/erosion effects unique to slug flow.

Figure 10 shows a SEM micrograph of a bubble impact point on the pipe wall under slug flow condition. The detailed description and analysis of the results are given by Vuppu and Jepson (1993). Figure 10 clearly shows the evidence of bubble impact and collapse on the corrosion film. It can be seen that there is a comparatively uniform protective inhibitor film around the impact crater. However, within the crater itself it is seen that the film has been ripped away from the wall and the corrosion deposits have flaked off. This can cause severe degradation of inhibitor performance under slug flow conditions. This type of mechanism is not seen in other flow regimes.

Kouba and Jepson<sup>9</sup> (1989) showed that the characteristics of slugs were determined by the dimensionless Froude number in the liquid film ahead of the slug. The Froude number for the film was defined as follows:

$$Fr_f = \frac{v_t - v_{LF}}{\sqrt{g h_{EFF}}} \quad (1)$$

where,  $v_t$  = translational velocity of the slug  
 $v_{LF}$  = velocity of the liquid film ahead of the slug  
 $h_{EFF}$  = effective height of the liquid film, calculated from the area of the liquid film divided by the width of the gas/liquid interface.

Figures 11 and 12 show the mixing zone at Froude numbers of 6 and 12 respectively. It is seen in Figure 11 that there is some turbulence in the slug at Froude number 6. There is still considerable entrainment

of gas. However, fewer gas bubbles reach the bottom of the pipe. Zhou and Jepson<sup>4</sup> (1994) indicate that relatively small amounts of gas are passed into the slug body. Figure 11 supports their studies. However, it is seen from Figure 12 that at Froude number 12, the turbulence levels increase dramatically, and the amount of gas entrained increases substantially. High resolution video of the slug indicates that the frequency of the generation of pulses of bubbles increases with Froude number.

Figure 13 shows a video image of ultrasonic signals obtained at Froude number 12. It clearly shows the high levels of turbulence associated with the mixing zone. At this Froude number, the gas bubbles do impact on the pipe wall. It appears that the ultrasonic signals indicate this mechanism as a function of Froude number in the slug.

Figure 14 through 16 show instantaneous fluctuations in shear stress at a distance of 20 cm into the mixing zone of the slug for a 60% oil-40 % saltwater mixture, at Froude numbers of 6, 9, and 12 respectively. It is seen that there is a significant increase in instantaneous shear stress values. At Froude number 6, the values range from 30 to 70 N/m<sup>2</sup>. These increase to about 80 to 120 N/m<sup>2</sup> at Froude number of 9. The maximum shear stress values at Froude number 12 are as high as 160 N/m<sup>2</sup>.

Figures 14, 15, and 16 also show the existence of definite peaks at regular frequency in the shear stress fluctuations. It is seen that both the intensity and frequency of the peaks increase with Froude number. There is some turbulent fluctuation in the values at Froude number 6. The levels of turbulence increase dramatically as the Froude number increases to 12. These results support the observations noted from the video images before.

Zhou and Jepson<sup>3</sup> (1993) also reported a dramatic rise in shear stress values across the slug front and into the mixing zone with an increase in oil percentage in the liquid from 20% to 60%. Zhou and Jepson<sup>4</sup> (1994) also discussed the effect of increasing void fraction at the bottom of the pipe on the corrosion rate. This is shown in Figure 17. A virtually linear relationship can be seen. Figure 18 shows the corrosion rate as a function of oil concentration for different Froude numbers. This was shown earlier by Zhou and Jepson<sup>4</sup> (1994). It can be seen that there are significant amounts of corrosion even for high oil cuts at higher Froude numbers.

The existence of the mixing vortex, the generation of pulses of gas bubbles, and the associated high levels of turbulence, scouring, and shear are mechanisms that are unique to slug flow. The result can be increased corrosion rates as seen in Figure 18.

## CONCLUSIONS

Video analysis has been conducted to examine the effects of flow parameters in the mixing zone on corrosion/erosion in horizontal slug flow. A multiphase mixture of an oil similar to that in gas condensate systems, and saltwater at compositions of 20%, 40%, 60%, and 80% were studied using carbon dioxide as the gas. The experiments were carried out at 0.137 MPa and 40C in 10 cm and 7.5 cm I.D. pipes.

The analysis clearly shows the existence of pulses of entrained gas bubbles in the mixing zone behind the front of the slug. At high Froude numbers these pulses of bubbles impact on the pipe wall and can collapse causing a cavitation-type effect, leading to highly increased corrosion rates seen in slug flow. The

mixing zone is also associated with a high degree of turbulence and wall shear.

Shear stress data obtained at high frequencies indicate the presence of large instantaneous peaks that seem to relate to the pulses of bubbles being generated. It is these instantaneous peaks that are more indicative of corrosion mechanisms in slug flow.

#### REFERENCES

- 1.) B. T. Ellison, C. J. Wen, American Institute of Engineers Symposium Series 77(1981): p. 161.
- 2.) J-Y Sun, W. P. Jepson, "Slug Flow Characteristics and their Effect on Corrosion Rates in Horizontal Oil and Gas Pipelines", SPE 1992, paper no. 24787, (Houston, TX: SPE, 1992).
- 3.) X. Zhou, W. P. Jepson, Proceedings of the 3rd International Offshore and Polar Engineering Conference, Singapore, Vol. 2 (1993): p. 161.
- 4.) X. Zhou, W. P. Jepson, "Corrosion in Three-Phase Oil/Water/Gas Slug Flow in Horizontal Pipes", Corrosion/94, paper no. 94026, (Houston, TX: NACE International, 1994).
- 5.) A. S. Green, B. V. Johnson, and H. Choi, "Flow-related Corrosion in Large Diameter Multiphase Flowlines", SPE 1989, paper no. 20685, (Houston, TX: SPE, 1989).
- 6.) A. E. Dukler, M. G. Hubbard, Industrial Engineering Chemistry Fundamentals 14, 4(1975): p. 337
- 7.) W. P. Jepson, Proceedings of the 3rd International Conference on Multiphase Flow, The Hague, Netherlands (1987): p. 187, (Cranfield, Bedford U. K.: BHRA, 1987).
- 8.) G. E. Kouba, W. P. Jepson, Proceedings of the 4th International Conference on Multiphase Flow, Nice, France (1989): p. 513.
- 9.) A. K. Vuppu, W. P. Jepson, "Study of Sweet Corrosion in Horizontal Multiphase Carbon Steel Pipeline", Offshore Technology Conference, paper no. 7494, (Houston, TX: SPE, 1994).

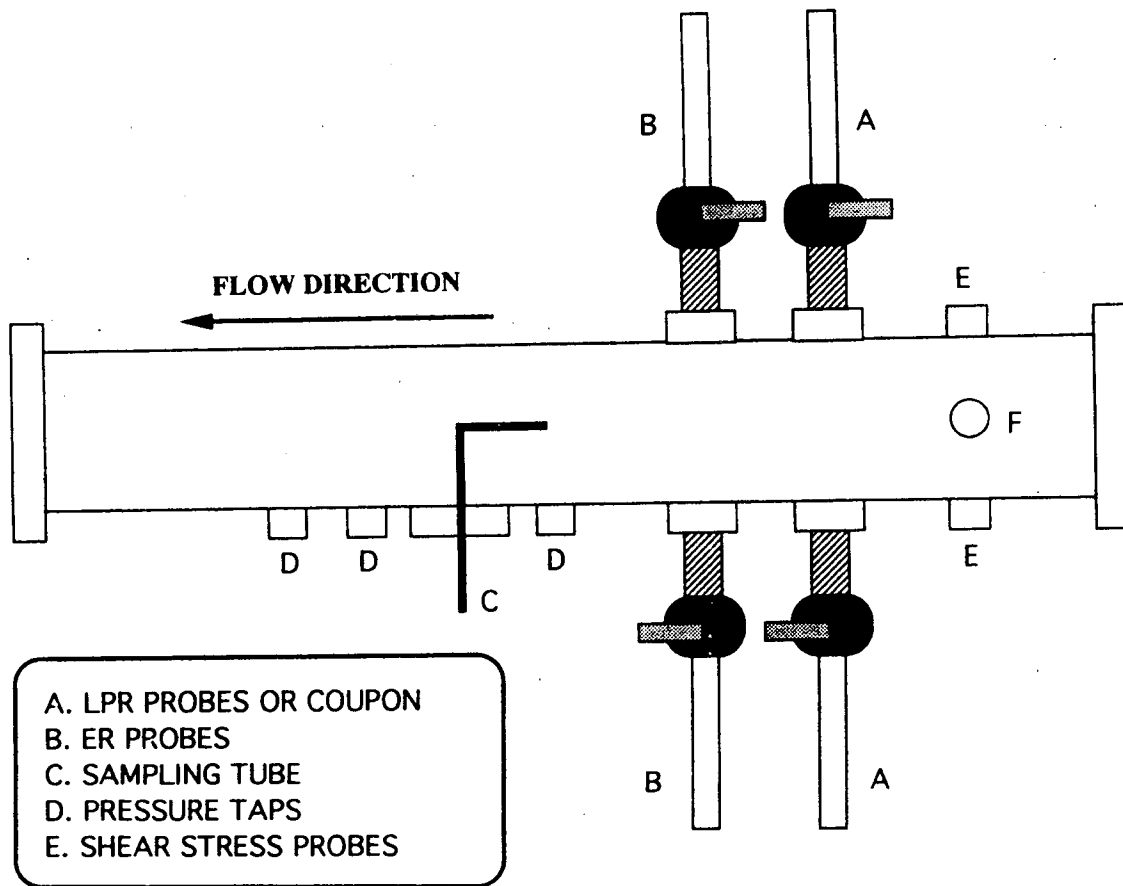


Figure 3: Test Section

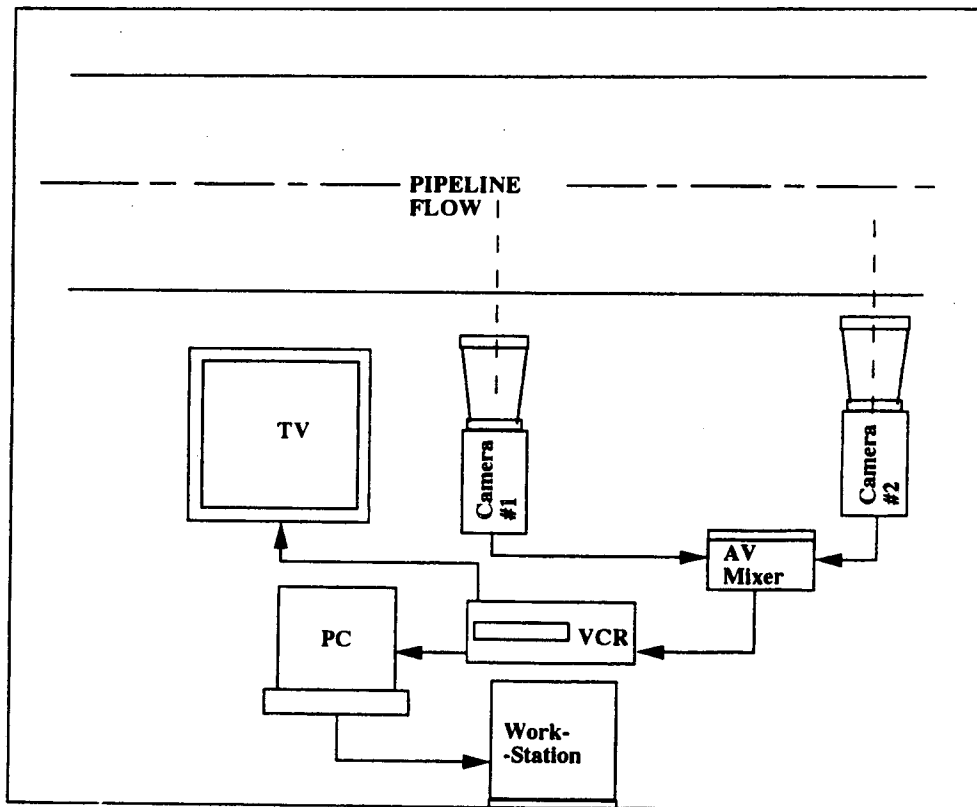


Figure 4: Schematic Diagram of Flow Visualization System

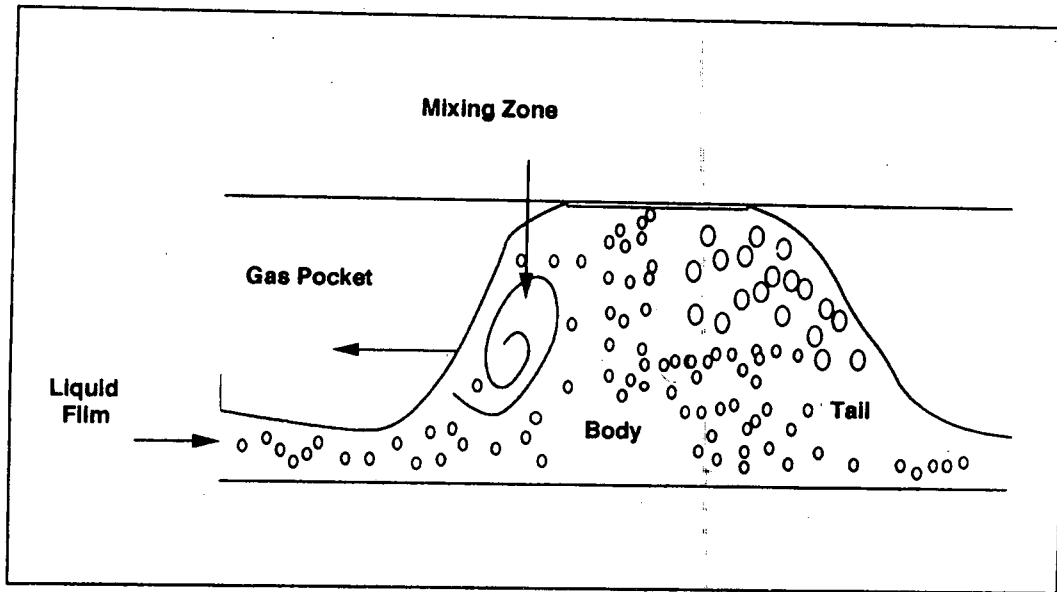
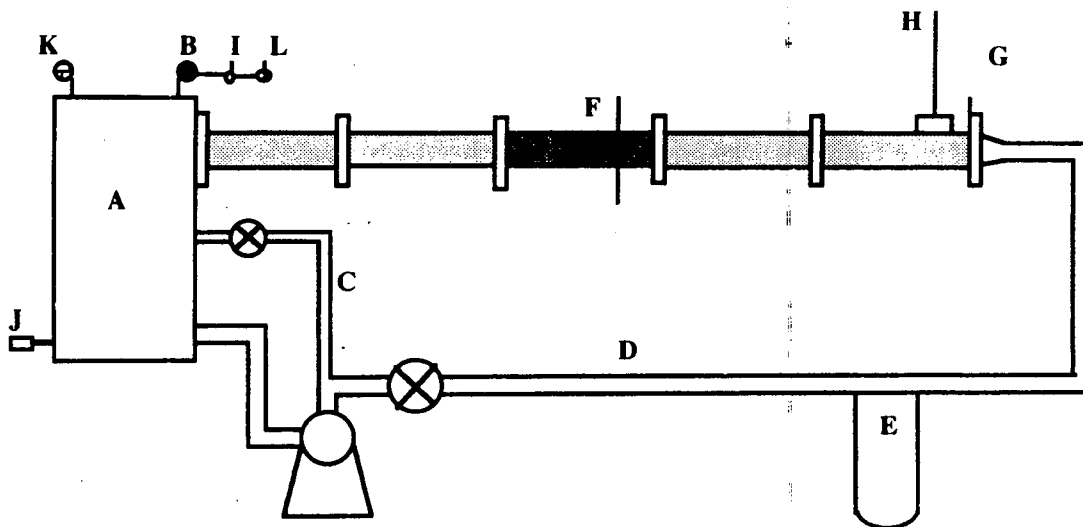


Figure 1: Profile of different regions of slug



- A. Liquid Tank
- B. Pressure Gauges
- C. Liquid Recycle
- D. Liquid Feed - 7.5 cm PVC
- E. Orifice Plate Manometer

- F. Test Section - 10 cm Plexiglass
- G. Flow Height Control Gate
- H. CO2 Feed Line
- I. VENT w/valve
- J. Heater
- K. Safety Valve
- L. Back Pressure Regulator

Figure 2: Layout of the experimental system

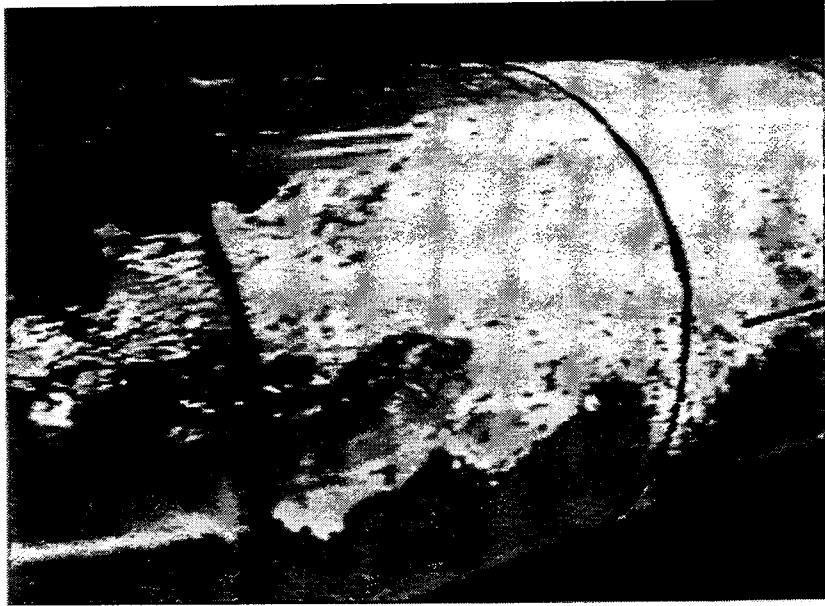


**Figure 5: Video image of slug front,  $t = 0$  s**

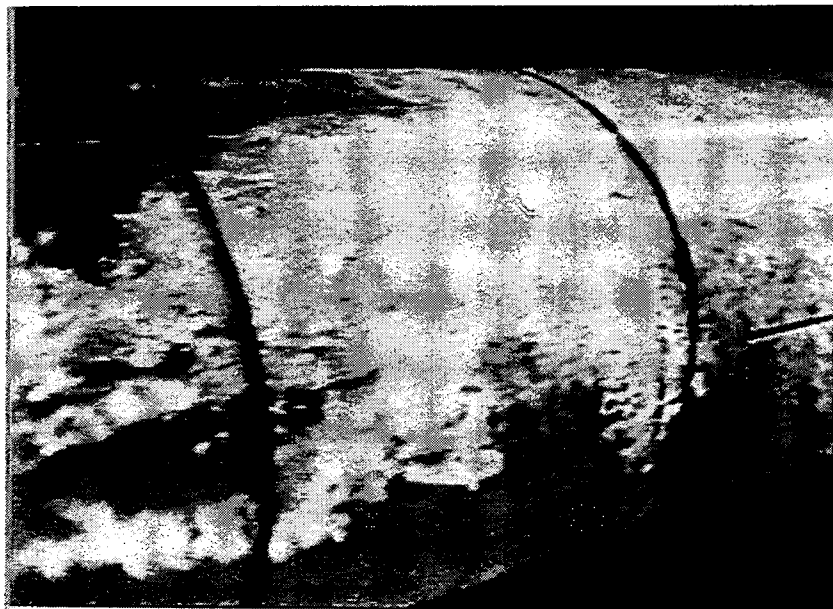


**Figure 6: Video image of slug front,  $t = 0.017$  s**

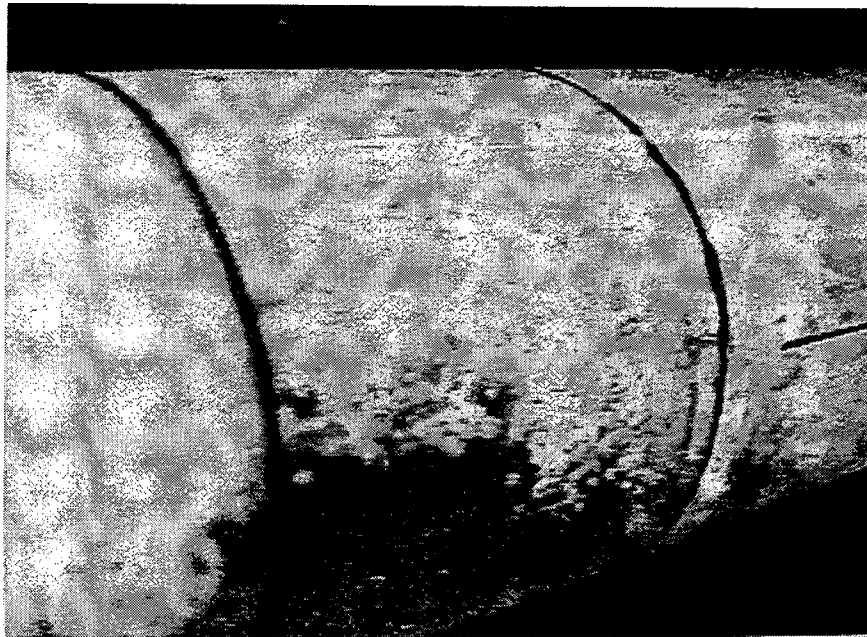


**Figure 7: Video image of mixing zone,  $t = 0.051$  s**

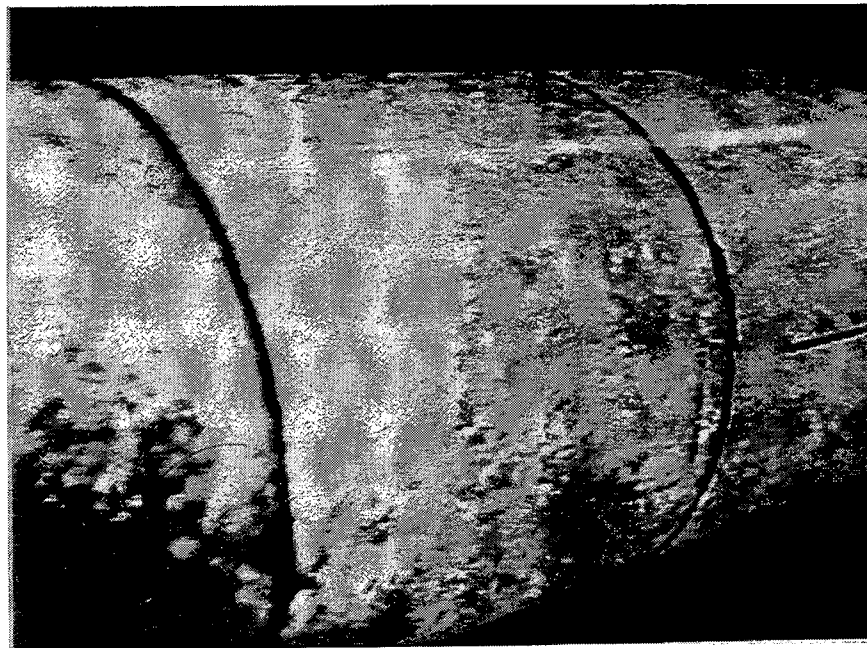


**Figure 8: Video image of mixing zone,  $t = 0.068$  s**

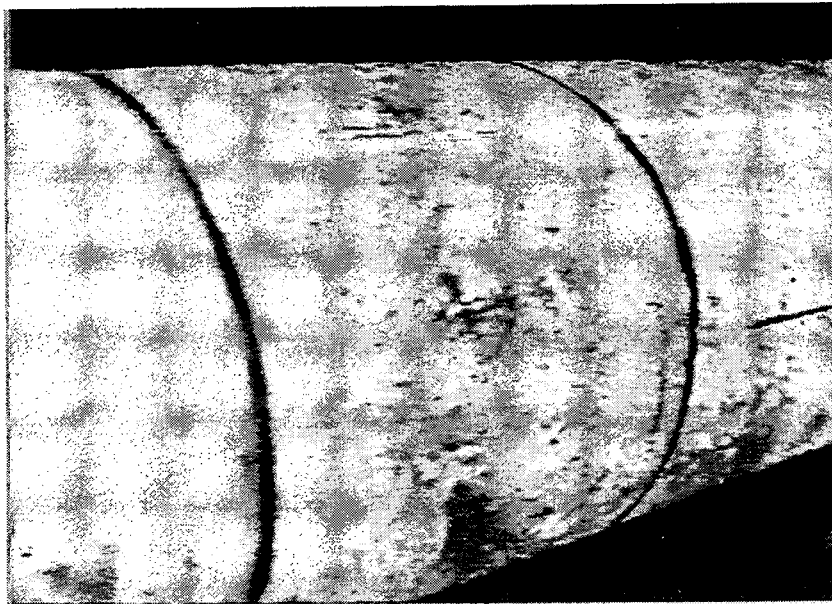


**Figure 9: Video image of mixing zone,  $t = 0.085$  s**

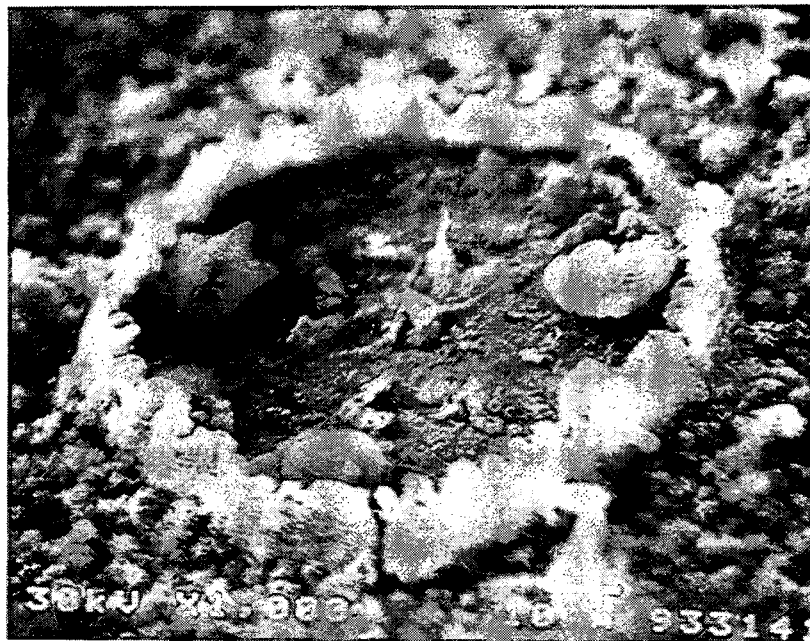


**Figure 10: Circular bubble impact points in the corrosion deposit observed for slug flow conditions. Compare the area inside and outside the bubble impact region**

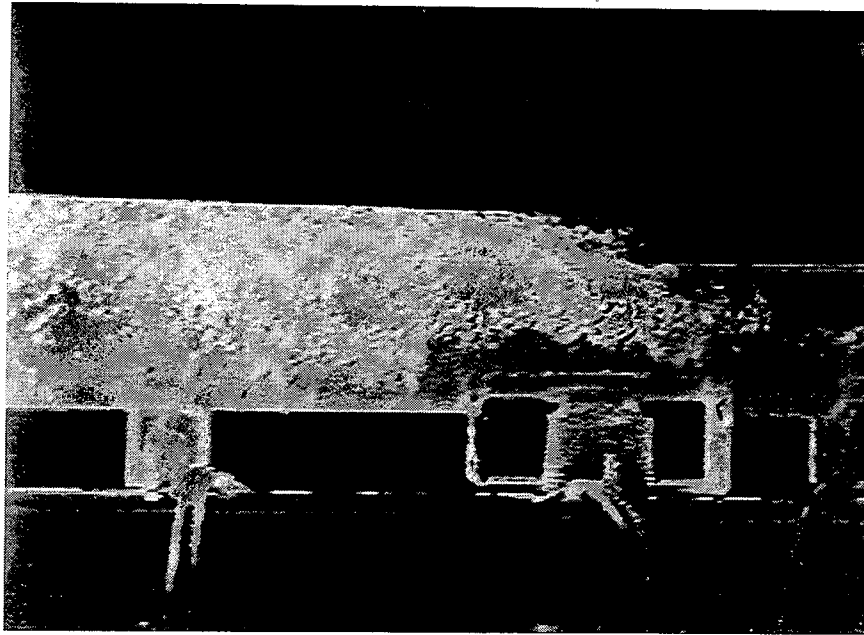


**Figure 11: Video image of mixing zone, Froude number = 6**

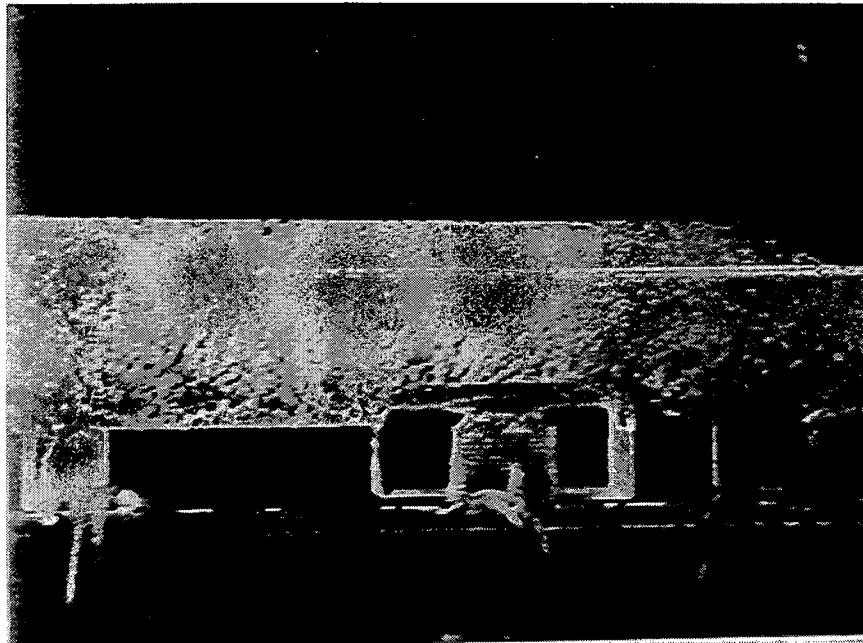


**Figure 12: Video image of mixing zone, Froude number = 12**

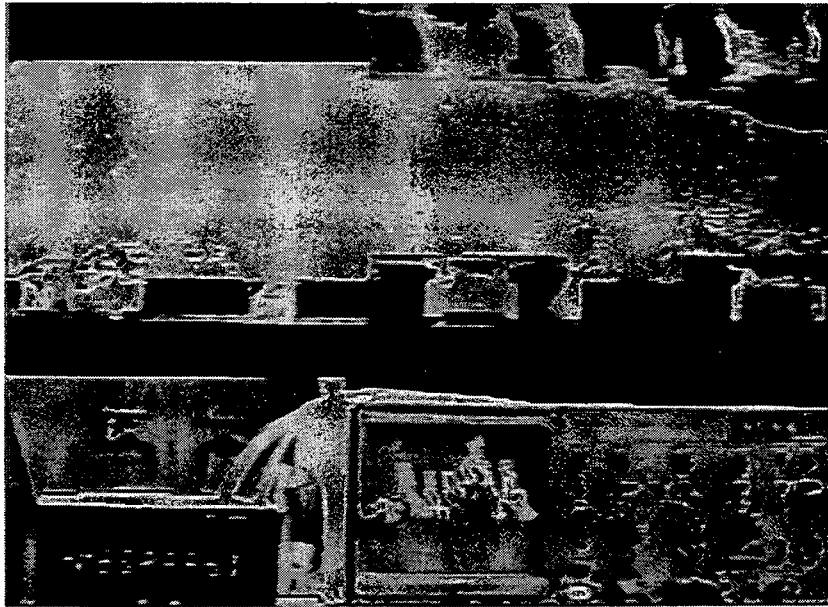


**Figure 13: Video image of ultrasonic signal response to mixing zone of slug**

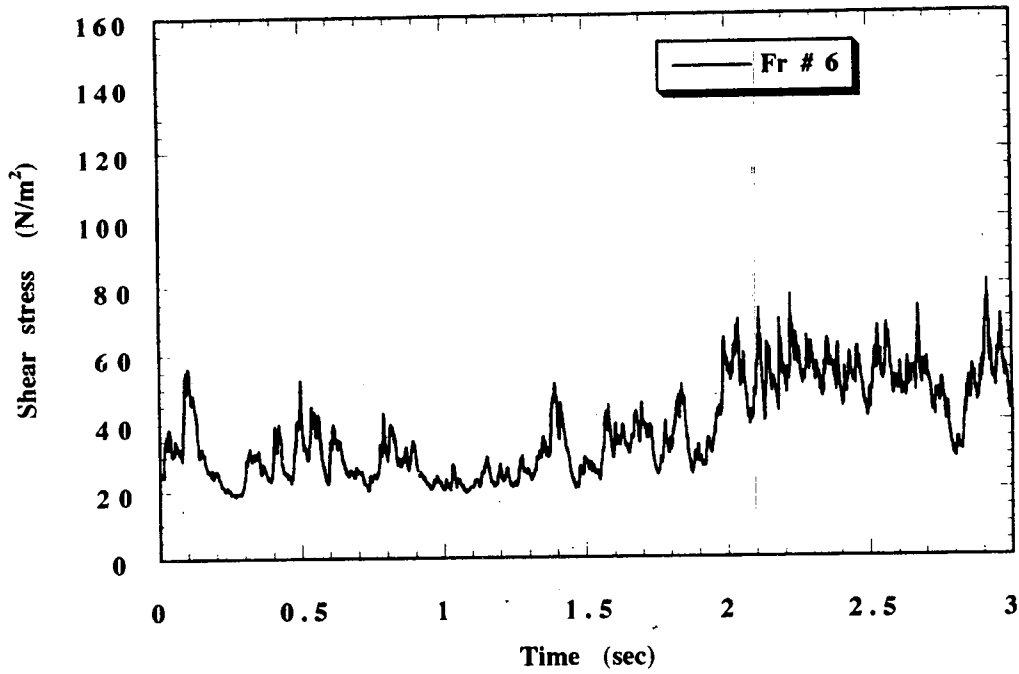


Figure 14: Variation in instantaneous shear stress at 20 cm from the slug front  
Salt water (40%), Oil (60%)

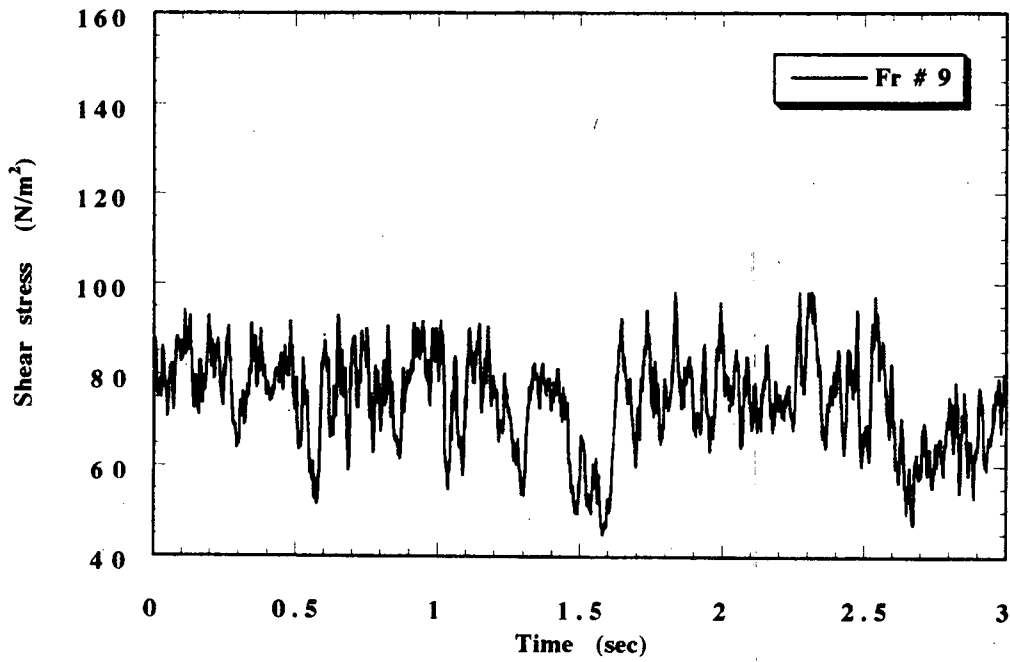


Figure 15: Variation in instantaneous shear stress at 20 cm from the slug front  
Salt water (40%), Oil (60%)

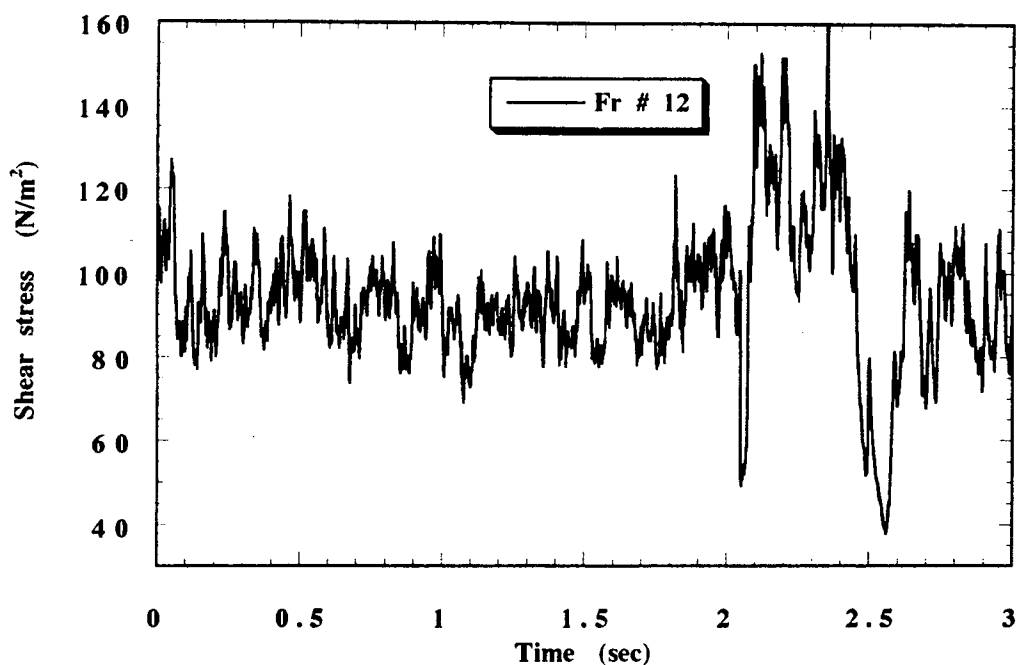


Figure 16: Variation in instantaneous shear stress at 20 cm from the slug front  
Salt water (40%), Oil (60%)

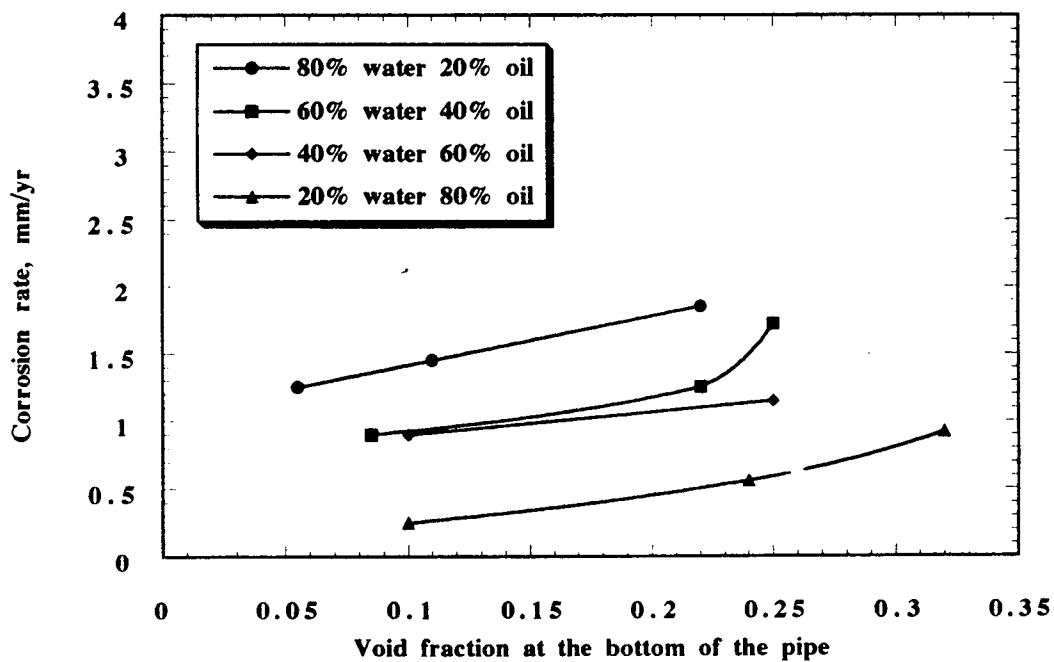


Figure 17: Effect of void fraction at the bottom of the pipe  
on corrosion rate

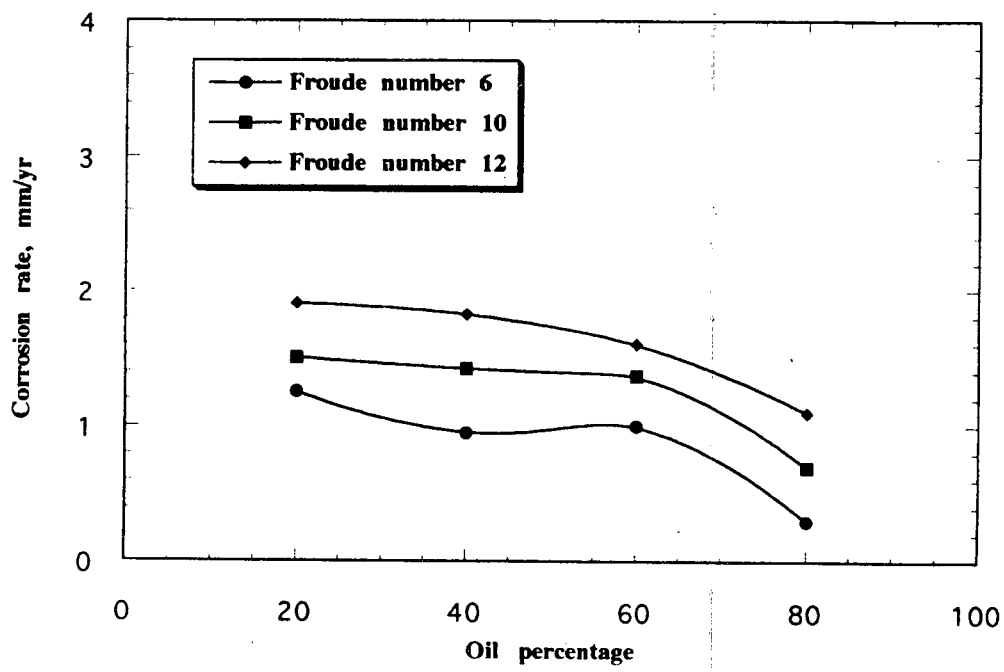


Figure 18: Effect of oil composition on corrosion rate